Heat shock protein 27 promotes cell cycle progression by down-regulating E2F transcription factor 4 and retinoblastoma family protein p130

Received for publication, April 5, 2018, and in revised form, August 23, 2018 Published, Papers in Press, August 30, 2018, DOI 10.1074/jbc.RA118.003310

Ah-Mee Park[‡1], **Ikuo Tsunoda**[‡], **and Osamu Yoshie**[‡§]

From the [‡]*Department of Microbiology, Kindai University Faculty of Medicine, Osakasayama, Osaka 589-8511, Japan and the* [§]*Health and Kampo Institute, 1-11-10 Murasakiyama, Sendai, Miyagi 981-3205, Japan*

Edited by Ursula Jakob

Heat shock protein 27 (HSP27) protects cells under stress. Here, we demonstrate that HSP27 also promotes cell cycle progression of MRC-5 human lung fibroblast cells. Serum starvation for 24 h induced G_1 arrest in these cells, and upon serum refeeding, the cells initiated cell cycle progression accompanied by an increase in HSP27 protein levels. HSP27 levels peaked at 12 h, and transcriptional up-regulation of six G_2/M-related genes (*CCNA2*, *CCNB1*, *CCNB2*, *CDC25C*, *CDCA3*, and *CDK1*) peaked at 24–48 h. siRNA-mediated HSP27 silencing in proliferating MRC-5 cells induced G_2 arrest coinciding with down-regulation of these six genes. Of note, the promoters of all of these genes have the cell cycle–dependent element and/or the cell cycle gene-homology region. These promoter regions are known to be bound by the E2F family proteins (E2F-1 to E2F-8) and retinoblastoma (RB) family proteins (RB1, p107, and p130), among which E2F-4 and p130 were strongly up-regulated in HSP27-knockdown cells. E2F-4 or p130 knockdown concomitant with the HSP27 knockdown rescued MRC-5 cells from G_2 arrest and up-regulated the six cell cycle genes. Moreover, we observed cellular senescence in MRC-5 cells on day 3 after the HSP27 knockdown, as evidenced by increased senescence-associated β-gal activity and up-regulated inflammatory cytokines. The cellular senescence was also suppressed by the concomitant knockdown of E2F-4/HSP27 or p130/HSP27. Our findings indicate that HSP27 promotes cell cycle progression of MRC-5 cells by suppressing expression of the transcriptional repressors E2F-4 and p130.

Heat shock protein 27 (HSP27),[2] also known as the heat shock protein family B member 1 (HSPB1), belongs to the small HSP family that commonly has a conserved C-terminal α-crystallin domain (1). In response to heat shock, HSP27 functions as an ATP-independent molecular chaperone to facilitate the proper refolding of damaged proteins (2). HSP27 is also involved in a wide range of cellular processes, such as cytoskeletal organization, redox metabolism, suppression of apoptosis, and cell proliferation (2–6). HSP27 also promotes degradation of ubiquitinated proteins by the 26S proteasome (7, 8). Furthermore, HSP27 is frequently overexpressed in cancer cells and closely associated with aggressive tumor behavior, metastasis, poor prognosis, and resistance to chemotherapy (9, 10).

Although the involvement of HSP27 in stressed cells and cancer cells is now well documented, there are only a few reports on the role of HSP27 in cell cycle progression and cellular senescence. For example, HSP27 reverses the G_2 arrest caused by HIV-1 viral protein R (11). HSP27 promotes G_1/S transition of cells arrested with serum depletion or with the nitric oxide donor glyceryl trinitrate by promoting ubiquitination and proteasomal degradation of the cyclin-dependent kinase (CDK) inhibitor $p27^{Kip1}$ (8). Embryonic fibroblasts derived from *Hspb1*-deficient mice display reduced entry into S phase with increased expression of the CDK inhibitors $p21^{Cip1}$ and $p27^{Kip1}$ (12). Taken together, HSP27 may have a promoting role in cell cycle progression. As for cellular senescence, HSP27 knockdown of MCF-7 mammary carcinoma cells led to reduced proliferation and acquisition of a spontaneous secretory phenotype, a feature of cellular senescence (13). Whereas overexpression of HSP27 protects MCF10A human mammary epithelial cells from doxorubicin-induced cellular senescence by inhibiting p53-mediated induction of $p21^{Cip1}$, the major regulator of the senescence program, depletion of HSP27 in HCT116 human colon carcinoma cells caused cellular senescence through activation of p53 and induction of $p21^{Cip1}$ (14). Thus, HSP27 may also have a suppressive role in cellular senescence by interfering with p53 activation and/or function.

Previously, we have demonstrated that HSP27 plays an essential role in transforming growth factor-β1–induced myofibroblast differentiation of normal lung fibroblasts and accordingly in the development of bleomycin-induced pulmonary

This work is supported by Grant-in-Aid for Scientific Research C JP15K08975 (B) (to A. M. P.), a grant from the Japan Science and Technology Agency (CREST Program) (to O. Y.), Novartis Pharma Research Grants 2017 (to A. M. P. and I. T.), and NIGMS, National Institutes of Health, COBRE Grant P30-GM110703 (to I. T.). The authors declare that they have no conflicts of interest with the contents of this article. The content is solely the responsibility of the authors and does not necessarily represent the official views of the National Institutes of Health.

This article contains Figs. S1–S4.

[1] To whom correspondence should be addressed: Dept. of Microbiology, Kindai University Faculty of Medicine, 377-2 Ohnohigashi, Osakasayama, Osaka 589-8511, Japan. Tel.: 81-72-366-0221; Fax: 81-72-366-0206; E-mail: ampk@med.kindai.ac.jp.

[2] The abbreviations used are: HSP, heat shock protein; CDK, cyclin-dependent kinase; FBS, fetal bovine serum; CDE, cycle-dependent element; CHR, cell cycle gene-homology region; RB, retinoblastoma; qPCR, quantitative PCR; mTOR, mammalian target of rapamycin; SASP, senescence-associated secretory phenotype; IL, interleukin; GAPDH, glyceraldehyde-3-phosphate dehydrogenase; CCK8, Cell Counting Kit-8.

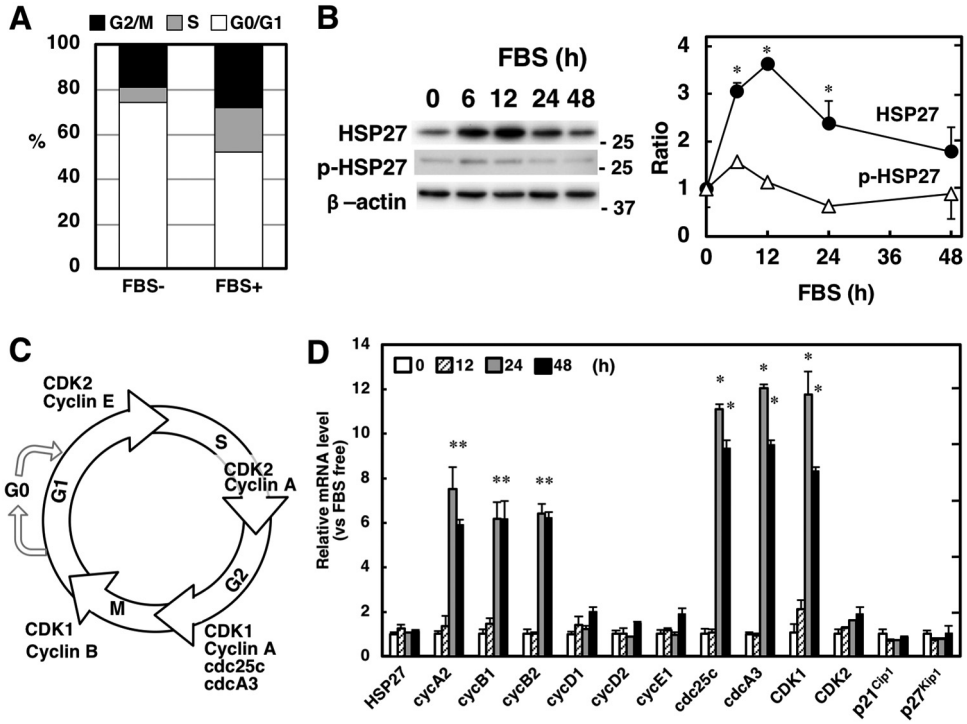

Figure 1. Up-regulation of HSP27 in serum-starved and -refed MRC-5. Cells were serum-starved for 24 h, refed with 5% FBS, and harvested at indicated time points. *A*, cell cycle analysis. Cells were serum-starved for 24 h and treated with or without FBS for 24 h. Cell cycles were determined using a MUSE cell analyzer. The representative results of four independent experiments are shown. *B*, immunoblot analysis. Protein levels of HSP27 and phospho-HSP27 were analyzed using an immunoblot analysis of cell lysates from control and FBS-treated MRC-5. For a loading control, β-actin was used. The representative results from four independent experiments are shown on the *left*. Quantitative data are shown on the *right* by mean ± S.E. (*error bars*) ($n = 4$). *, $p < 0.05$. *C*, a depiction of the cell cycle with cyclins, CDKs, and related molecules involved in each cell cycle phase. *D*, expression of cell cycle regulatory genes. RNAs were isolated from cells treated with FBS for 0 h (*open*), 12 h (*hatched*), 24 h (*gray*), or 48 h (*closed*). The relative expression levels of cell cycle regulatory genes were determined using qPCR with GAPDH as an internal control for normalization. *, $p < 0.05$ *versus* without FBS (0 h).

fibrosis (15). During the same study, we also observed that siRNA knockdown of HSP27 significantly suppressed cell proliferation of normal lung fibroblasts. Thus, in the present study, we further explored the role of HSP27 in cell cycle progression by using MRC-5, a normal human lung fibroblast cell line (16). MRC-5 was serum-starved and -refed to synchronize the cell cycle. Upon refeeding, we found a rapid increase in HSP27 protein along with transcriptional up-regulation of six G_2/M-related genes: *CCNA2* (cyclin A2), *CCNB1* (cyclin B1), *CCNB2* (cyclin B2), *CDC25C*, *CDCA3*, and *CDK1* (17, 18). We further found that HSP27 knockdown of proliferating MRC-5 induced G_2 arrest together with down-regulation of the same six genes and up-regulation of E2F-4/p130. We demonstrated that concomitant knockdown of E2F-4 or p130 with HSP27 knockdown rescued MRC-5 from G_2 arrest and also prevented the down-regulation of the six genes. MRC-5 also underwent cellular senescence 3 days after HSP27 knockdown as evidenced by increases in senescence-associated β-galactose positivity and up-regulation of proinflammatory cytokines. The cellular senescence was also prevented by the concomitant knockdown of E2F-4 or p130 with HSP27 knockdown. Collectively, HSP27 plays a pivotal role in cell cycle progression of MRC-5 by down-regulating the expression of E2F-4/p130, whose up-regulation leads to G_2 arrest through down-regulation of the six G_2/M-related genes, which eventually results in cellular senescence in MRC-5.

Results

HSP27 increases during cell cycle progression of serum-refed MRC-5

MRC-5 is a human diploid lung fibroblast cell line that is widely used as a model of normal human fibroblasts (15, 16). In our preliminary experiments, HSP27 knockdown by siRNA transfection significantly suppressed cell proliferation of MRC-5 (data not shown, but see Fig. 2). To test whether HSP27 was involved in cell cycle progression, we used the technique of serum starvation and refeeding to synchronize the cell cycle of MRC-5. After 24 h of fetal bovine serum (FBS) starvation, we refed MRC-5 with 5% FBS to initiate the cell cycle progression. We confirmed that whereas FBS starvation increased cells at G_0/G_1 phase ($G_0/G_1 = 73 \pm 0.6\%$, $S = 6 \pm 0.2\%$, $G_2/M = 20 \pm 0.5\%$), FBS refeeding increased cells at S and G_2/M phases ($G_0/G_1 = 52 \pm 0.7\%$, $S = 20 \pm 0.2\%$, $G_2/M = 28 \pm 0.5\%$) (Fig. 1*A*). We found that FBS refeeding also increased the protein level of HSP27 with a peak at 12 h (Fig. 1*B*). No significant increase was seen in the phosphorylation of HSP27 (Fig. 1*B*). Because cell cycle progression is regulated by cyclins and CDKs (Fig. 1*C*), we quantified mRNA levels of these molecules together with that of HSP27 (Fig. 1*D*). We found that HSP27 mRNA was not up-regulated by FBS refeeding. Thus, the increase of HSP27 protein was mostly translationally and/or post-translationally controlled in FBS-refed MRC-5. On the other hand, among the 12 cell cycle–related genes examined,

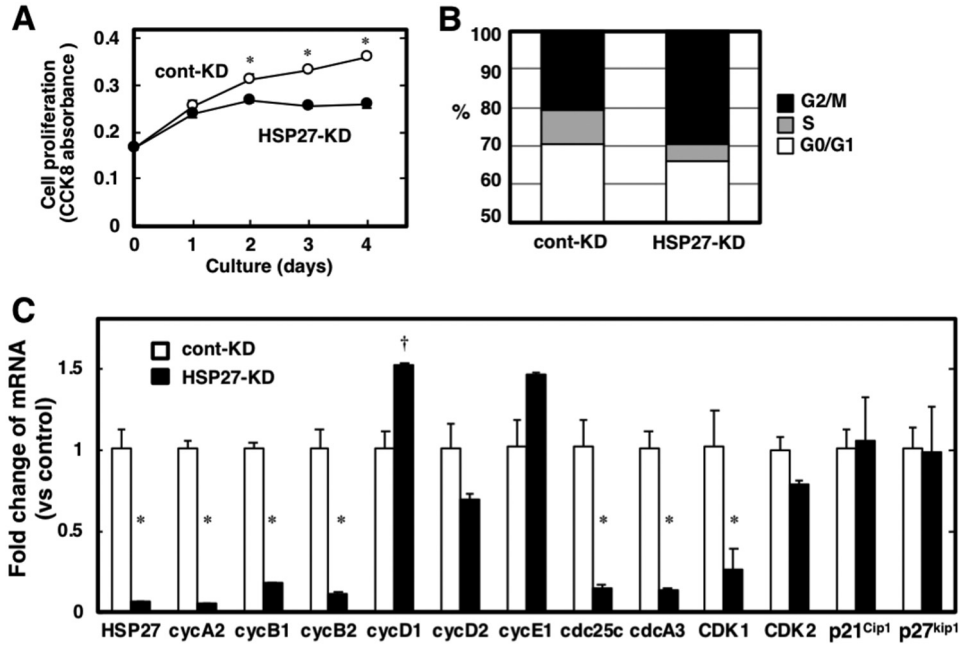

Figure 2. Cell cycle arrest by HSP27 knockdown. Cells were transfected with control siRNA (*cont-KD*) or HSP27 siRNA (*HSP27-KD*). *A*, cell proliferation. The CCK8 kit was used to monitor cell proliferation. *Open* and *closed circles* indicate control siRNA– and HSP27 siRNA–transfected cells, respectively. Data are shown as mean ± S.E. (*error bars*) ($n = 6$). *, $p < 0.05$. *B*, cell cycle analysis. Two days after siRNA transfection, cell cycles were determined using a MUSE cell analyzer. The representative results of four independent experiments are shown. *C*, expression of cell cycle regulatory genes. Two days after siRNA transfection, the relative expression levels of the indicated cell cycle regulatory genes were determined using qPCR with GAPDH as an internal control for normalization. *, $p < 0.05$ *versus* control (decrease); †, $p < 0.05$ *versus* control (increase).

the six genes (cyclin A2, cyclin B1, cyclin B2, cdc25c, cdcA3, and CDK1) were strongly up-regulated after 24–48 h of FBS refeeding (Fig. 1*D*). No such changes were seen in the mRNA levels of cyclin D1, cyclin D2, cyclin E1, CDK2, and the two CDK inhibitors $p21^{Cip1}$ and $p27^{Kip1}$. Of note, all of the six up-regulated genes are those involved in the G_2/M phases and contain the cell cycle-dependent element (CDE) and/or the cell cycle gene-homology region (CHR) in their promoters (19); *CCNA2*, *CDC25C*, *CDCA3*, and *CDK1* have both CDE and CHR, whereas *CCNB1* and *CCNB2* have CHR. These elements are known to be regulated by the binding of the E2F and retinoblastoma (RB) family proteins (19, 20).

HSP27 knockdown induces G_2 arrest

To examine the role of HSP27 in the cell cycle progression of MRC-5, we next performed HSP27 knockdown experiments using siRNA transfection. As shown in Fig. 2*A*, HSP27 knockdown significantly decreased cell proliferation. This was not due to increased cell death (percentage of dead cells as follows: control knockdown, 3.0 ± 0.4; HSP27 knockdown, 2.4 ± 0.4). Furthermore, as shown in Fig. 2*B*, HSP27 knockdown significantly increased cells at G_2/M phase ($G_0/G_1 = 66 \pm 0.1\%$, $S = 4 \pm 0.5\%$, $G_2/M = 30 \pm 0.4\%$) compared with control knockdown ($G_0/G_1 = 70 \pm 0.7\%$, $S = 9 \pm 0.3\%$, $G_2/M = 21 \pm 0.2\%$) (Fig. 2*B*). Although cells at G_2 and M are diploid and indistinguishable by propidium iodide staining, M-phase cells can be distinguished by phosphohistone H3 positivity (21). Because HSP27 knockdown did not increase cells positive for phosphohistone H3 (data not shown), the cell cycle arrest was mainly at G_2. We also examined the viability of cells by using the Muse Count & Viability Kit. No significant difference in dead cell count was found between cells transfected with HSP27 siRNA (2.4 ± 0.4%) and control siRNA (3.0 ± 0.4%) ($p = 0.29$). Thus, we concluded that HSP27 knockdown induced G_2 arrest in MRC-5.

HSP27 knockdown induces down-regulation of the six cell cycle regulatory genes

HSP27 knockdown efficiently decreased not only HSP27 mRNA but also the mRNAs of the six cell cycle regulatory genes that were up-regulated in FBS-refed MRC-5: cyclin A2, cyclin B1, cyclin B2, cdc25c, cdcA3, and CDK1 (Fig. 2*C*). On the other hand, although cyclin D1 mRNA was significantly up-regulated by HSP27 knockdown, the mRNA levels of cyclin D2, cyclin E1, and CDK2 as well as those of the two CDK inhibitors $p21^{Cip1}$ and $p27^{Kip1}$ were not affected by HSP27 knockdown. These results suggested that HSP27 was involved in the up-regulation of the six G_2/M cell cycle progression molecules in MRC-5.

E2F-4 and p130 increase by HSP27 knockdown

As mentioned earlier, the six genes (*CCNA2*, *CCNB1*, *CCNB2*, *CDC25C*, *CDCA3*, and *CDK1*) that were down-regulated by HSP27 knockdown commonly carry the CDE/CHR or CHR element in their promoters (19). Thus, their expression can be regulated by the E2F family proteins and RB family proteins (RB1, p107, and p130) that bind to these elements (19, 20). Among the E2F family proteins, E2F-1 to E2F-3 positively and E2F-4 to E2F-8 negatively regulate the cell cycle (19). Because the HSP27 knockdown strongly decreased the expression of the six genes, we quantified the mRNA levels of the repressor E2F family proteins in MRC-5 upon HSP27 knockdown. By using qPCR, we found that the expression of E2F-4 was significantly increased upon HSP27 knockdown (Fig. 3*A*), whereas the expression of E2F-5 to E2F-8

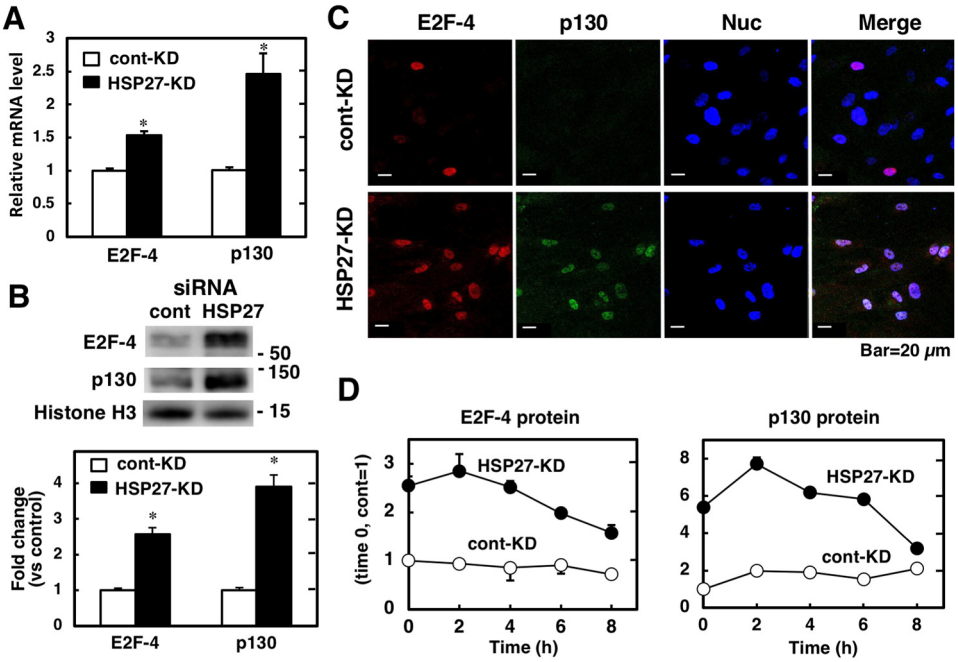

Figure 3. HSP27 knockdown up-regulates E2F-4 and p130 expression. *A*, quantitative PCR. The relative expression levels of E2F-4 and p130 genes were determined using qPCR with GAPDH as an internal control for normalization. *, $p < 0.05$. *B*, immunoblot analysis. Protein levels of E2F-4 and p130 in nuclear extracts from cells transfected with control or HSP27 siRNA were determined by immunoblot analysis. For a loading control, histone H3 was used. Quantitative data are shown as mean ± S.E. (*error bars*) ($n = 4$). *, $p < 0.05$. *C*, immunofluorescence staining. Cells were transfected with control siRNA or HSP27 siRNA and cultured for 48 h. Immunofluorescence staining was performed for E2F-4 (*red*) and p130 (*green*). Nuclear staining was performed with To-Pro3 (*blue*). *Scale bar*, 20 μm. *D*, protein-chasing experiment. Cells were transfected with control or HSP27 siRNA. After 48 h, cells were treated with 20 μM cycloheximide. Cell lysates were prepared at the indicated time points. Immunoblot analysis was performed for E2F-4 and p130. Signal intensities were measured with ImageJ software. Data are shown as mean ± S.E. ($n = 4$). *, $p < 0.05$.

was negligible in MRC-5 (data not shown). Among the RB family proteins, HSP27 knockdown increased the expression of p130 (Fig. 3*A*) but not RB1 (Fig. S1), whereas the mRNA level of p107 was quite low in this cell line regardless of HSP27 knockdown (Fig. S1). We also confirmed strong increases of E2F-4 and p130 proteins by HSP27 knockdown using immunoblot analysis (Fig. 3*B*) and immunocytochemistry (Fig. 3*C*).

To examine whether HSP27 could directly interact with E2F-4 and/or p130, we conducted co-immunoprecipitation experiments and found no evidence for the direct binding of HSP27 to E2F-4 or p130 (data not shown). Because HSP27 was reported to enhance ubiquitination and degradation of intracellular proteins such as $p27^{Kip1}$ and IκB (7, 8), we also conducted the protein chase experiment using cycloheximide to determine the effect of HSP27 knockdown on the half-life of E2F-4 and p130. Although we expected slower degradation of E2F-4 and/or p130 by HSP27 knockdown, we actually found enhanced degradation of E2F-4 and p130 by HSP27 knockdown compared with control knockdown (Fig. 3*D*).

E2F-4 knockdown rescues G_2 arrest by HSP27 knockdown

To determine the role of E2F-4 in the G_2 arrest of MRC-5 by HSP27 knockdown, we performed single and double knockdown experiments. Immunoblot analysis confirmed the efficient knockdown of HSP27 and E2F-4 by HSP27 siRNA and E2F-4 siRNA, respectively (Fig. 4*A*). Whereas the single knockdown of HSP27 decreased cell number (Fig. 4*B*) and induced G_2 arrest (Fig. 4*C*), the single knockdown of E2F-4 had no such effect on cell number (Fig. 4*B*) or cell cycle progression (Fig. 4*C*). However, the double knockdown of HSP27 and E2F-4 reversed the effect of HSP27 knockdown on cell number (Fig. 4*B*) and G_2 arrest (Fig. 4*C*). Furthermore, among the six G_2/M regulatory genes that were down-regulated by HSP27 knockdown, the down-regulations of at least cyclin B2, cdc25c, cdcA3, and CDK1 were significantly prevented by the concomitant knockdown of E2F-4 (Fig. 4*D*). These results suggested that up-regulation of E2F-4 was mostly responsible for the G_2 arrest induced by HSP27 knockdown.

p130 knockdown also rescues G_2 arrest by HSP27 knockdown

We next performed similar experiments for p130. Immunoblot confirmed efficient knockdown of HSP27 and p130 by HSP27 siRNA and p130 siRNA, respectively (Fig. 4*E*). We also observed that the concomitant knockdown of p130 rescued the effect of HSP27 knockdown on cell number (Fig. 4*F*) and cell cycle (Fig. 4*G*). However, because p130 is a general cell cycle repressor, the single knockdown of p130 significantly increased cell numbers (Fig. 4*F*). Furthermore, by qPCR, we found that single p130 knockdown significantly up-regulated mRNAs for HSP27, cyclin A2, cyclin B1, cyclin B2, cdc25c, and cdcA3 (Fig. 4*H*). Since the HSP27/p130 double knockdown led to a similar level of HSP27 as control cells, but a lower level of p130 expression, this might allow us to assess the effect of low p130 without a significant change in the level of HSP27. Thus, the reduction of p130 alone led to the up-regulation of the six cell cycle–associated genes.

HSP27 knockdown leads to cellular senescence

We also examined a long-term effect of HSP27 knockdown on MRC-5. After 3 days of HSP27 knockdown, we observed

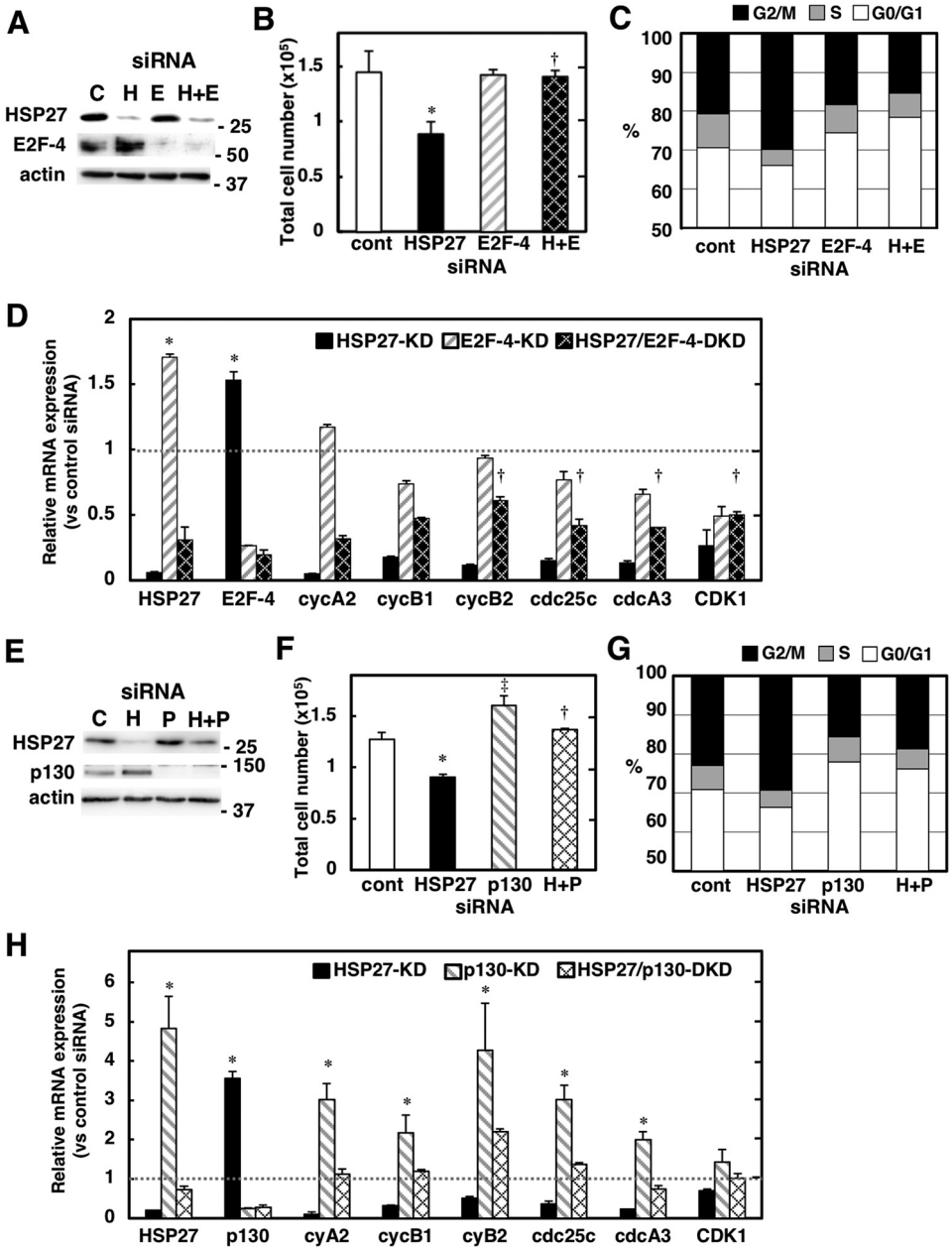

Figure 4. E2F-4/p130 mediates cell cycle arrest by HSP27 knockdown. Cells were transfected with control siRNA, HSP27 siRNA, E2F-4 siRNA, and/or p130 siRNA as indicated and cultured for 48 h. *A* and *E*, immunoblot analysis. Protein levels of HSP27, E2F-4, or p130 in cell lysates were determined by immunoblot analysis. For a loading control, β-actin was used. *B* and *F*, total cell numbers. * and ‡, $p < 0.05$ *versus* control siRNA; †, $p < 0.05$ *versus* HSP27 siRNA. *C* and *G*, cell cycle analysis. *D* and *H*, expression of cell cycle regulatory genes. qPCR was performed with GAPDH as an internal control for normalization. †, $p < 0.05$ *versus* HSP27 siRNA; *, $p < 0.05$ *versus* control siRNA. *Error bars*, S.E.

significant increases in cells positive for senescence-associated β-gal (SA-β-gal) (Fig. 5*A*) and significant up-regulation of pro-inflammatory cytokines IL-1α and IL-8 (Fig. 5*B*). These results demonstrated that HSP27 knockdown of MRC-5 induced not only cell cycle arrest but also cellular senescence after day 3. Again the concomitant knockdown of E2F-4 or p130 with HSP27 knockdown effectively prevented the increase of β-gal–positive cells. Of note, although HSP27 knockdown significantly decreased the mRNA level of p16, a senescence inducer molecule (22), it did not affect the protein level of p16 (Fig. 5*C*).

HSP27 knockdown induces cellular senescence in G_2-arrested cells

Because HSP27 knockdown induced G_2 arrest, we also examined whether increased cellular senescence by HSP27 knockdown could also be associated with the G_2 phase, whose cells can be identified by intense Ki-67–positive nuclear staining and/or cytoplasmic cyclin B1 staining (23, 24). In control-knockdown cells, SPiDER-βGal®–positive senescent cells were negative for Ki-67 (Fig. 5*B*) or cytoplasmic cyclin B1 (data not shown). On the other hand, in HSP27-knockdown cells, we found that some SPiDER-βGal®–positive senescent cells had

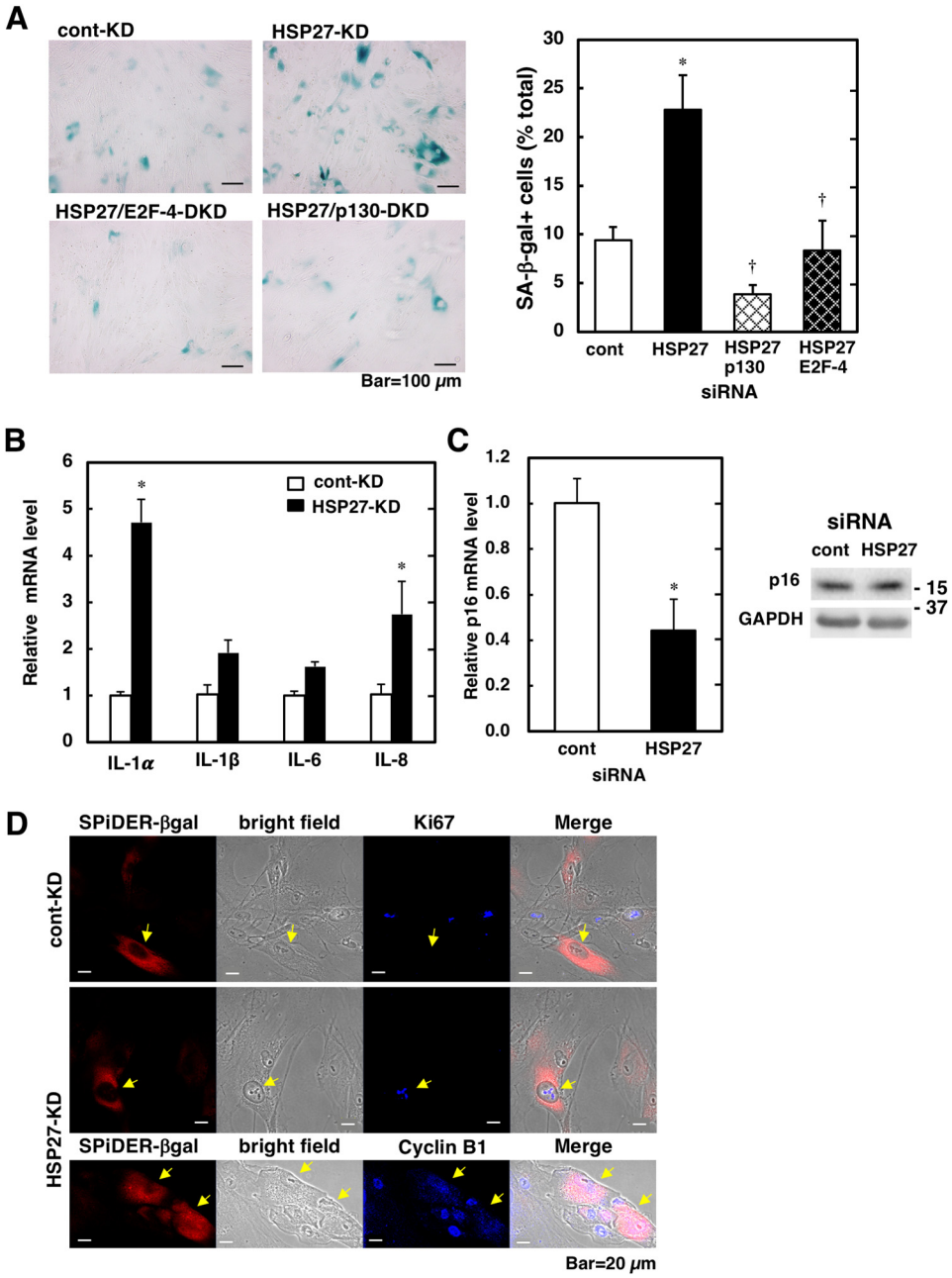

Figure 5. Cellular senescence induced by HSP27 knockdown. *A*, β-gal staining. Cells were transfected with control siRNA, HSP27 siRNA, HSP27 siRNA + p130 siRNA, or HSP27 siRNA + E2F-4 siRNA. Three days after transfection, cells were fixed with 4% paraformaldehyde, stained for β-gal (*blue*), and counterstained with 4′,6-diamidino-2-phenylindole. Total cells and cells positive for β-gal were analyzed by ImageJ software. The representative results are shown on the *left*. Quantitated data are shown on the *right* as mean ± S.E. (*error bars*) ($n = 4$). *, $p < 0.05$ *versus* control siRNA; †, $p < 0.05$ *versus* HSP27 siRNA. *B*, expression of pro-inflammatory cytokines. Three days after siRNA transfection, the relative expression levels of proinflammatory cytokines were determined by qPCR. *, $p < 0.05$ *versus* control siRNA. *C*, expression of p16. The mRNA and protein levels of p16 were determined by qPCR (*left*) and immunoblot assay (*right*), respectively, with GAPDH as the internal control for normalization. Data are shown as mean ± S.E. ($n = 4$). *, $p < 0.05$. *D*, cell cycle analysis of senescent cells. Control siRNA– or HSP27 siRNA–transfected cells were reseeded in an 8-well chamber slide after a 24-h culture. Three days after transfection, cells were fixed with 4% paraformaldehyde and stained with SPiDER-βGal (*red*), followed by immunofluorescence staining with antibody against Ki-67 (*blue*) or cyclin B1 (*blue*). *Scale bar*, 20 μm. *Arrows*, senescence cells.

Ki-67–positive nucleoli or cyclin B1–positive cytoplasm, suggesting that increased senescent cells in HSP27 knockdown were mostly at the G_2 phase (Fig. 5*D*).

Cell cycle arrest by HSP27 knockdown is not associated with oxidative cellular damage

Cell cycle arrest occurs under unfavorable conditions, such as nutrient deficiency or DNA damage. Because we used MRC-5 maintained in 5% FBS-Opti-MEM in HSP27-knockdown experiments, the nutrient deficiency might not be the likely cause of the cell cycle arrest. On the other hand, because HSP27 has an antioxidant property (2), oxidative damage might be increased by HSP27 knockdown, thereby leading to DNA damage and cell cycle arrest. To test this possibility, we analyzed protein oxidation, protein ubiquitination, and DNA damage in HSP27-knockdown MRC-5. We found no apparent

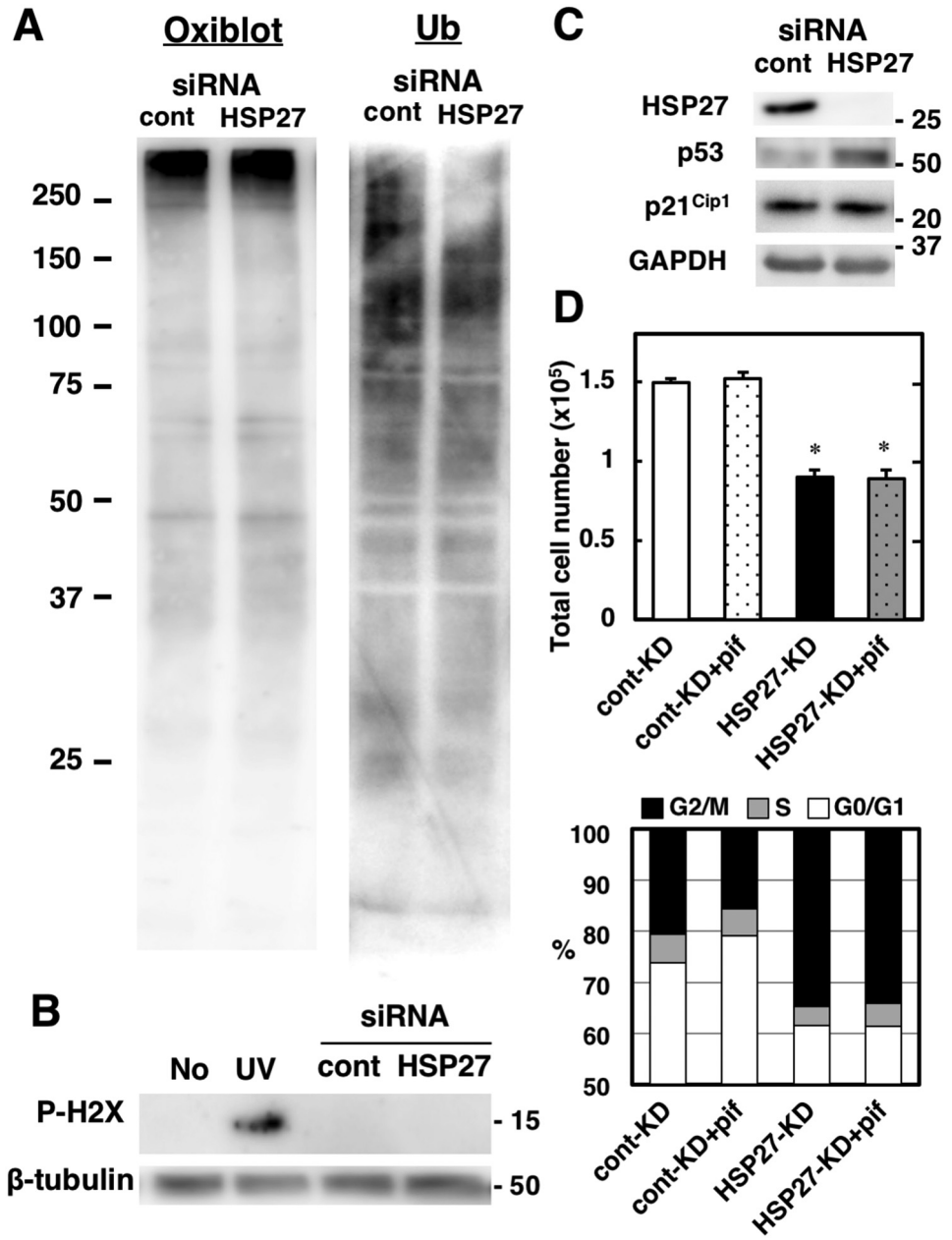

Figure 6. Analysis of oxidative cell damage. Cells were transfected with control siRNA (*cont*) or HSP27 siRNA (*HSP27*). *A*, protein oxidation and ubiquitination. These were determined by Oxiselect™ protein carbonylation immunoblot kit and immunoblot analysis with anti-ubiquitin antibody, respectively. *B*, DNA damage analysis. Immunoblot analysis was performed for a DNA damage marker phosphohistone 2X (*P-H2X*). Cells treated with UV light were used as a positive control (*UV*). *C*, immunoblot analysis. Protein levels of p53 and $p21^{Cip1}$ in cell lysates were determined by immunoblot analysis. GAPDH shown as a loading control is identical to that of Fig. 5*C*. *D*, effect of pifithrin-α, a p53 inhibitor. One day after control siRNA or HSP27 siRNA transfection, cells were incubated with or without 10 μM pifithrin-α (*pif*) for 24 h. Cell number and cell cycle were determined using a MUSE cell analyzer. Cell number data are shown as mean ± S.E. (*error bars*) ($n = 4$). *, $p < 0.05$. The representative cell cycle results of four independent experiments are shown.

increases in protein oxidation or ubiquitination by HSP27 knockdown (Fig. 6*A*). The phosphohistone 2X, a marker of cellular DNA damage, was also not increased by HSP27 knockdown either (Fig. 6*B*). Thus, oxidative damage was not the likely cause of the cell cycle arrest induced by HSP27 knockdown.

Cell cycle arrest by HSP27 knockdown is independent of p53

We further examined the possible involvement of p53, a key molecule of cell cycle arrest (25). Although p53 was increased by HSP27 knockdown, $p21^{Cip1}$, the CDK inhibitor and one of the major downstream mediators of p53 function, was not affected (Fig. 6*C*). In addition, pifithrin-α, a p53 inhibitor (26), did not prevent the decrease in cell number or cell cycle arrest by HSP27 knockdown (Fig. 6*D*). Pifithrin-α also did not prevent the down-regulation of mRNA levels of the cell cycle–associated genes by HSP27 knockdown either (data not shown). We concluded that the cell cycle arrest induced by HSP27 knockdown was mostly independent of p53.

Discussion

The cell cycle is a process composed of four phases: G_1 (pre-DNA synthesis), S (DNA synthesis), G_2 (pre-division), and M

(mitosis) (27, 28). Cyclins, CDKs, and CDK inhibitors ($p21^{Cip1}$ and $p27^{Kip1}$) are the key molecules that directly regulate the cell cycle progression (Fig. 1*C*) (17, 27). The E2F family of transcription factors also control the cell cycle at the transcriptional level as activators (E2F-1 to E2F-3) or repressors (E2F-4 to E2F-8) (29). The repressor proteins, especially E2F-4 and E2F-5, are known to function in association with the RB proteins (30, 31).

In the present study, we used MRC-5, a normal human lung fibroblast cell line (16), and demonstrated a rapid increase in HSP27 protein with a peak at 12 h in serum-starved and -refed MRC-5 (Fig. 1). Furthermore, the six genes associated with G_2/M cell cycle progression (*CCNA2*, *CCNB1*, *CCNB2*, *CDC25C*, *CDCA3*, and *CDK1*) were strongly up-regulated in serum-refed MRC-5 (Fig. 1). Of note, all these six genes carry CDE and/or CHR in their promoters, where the complex of a repressive E2F and RB family proteins is known to bind (19, 20). By using the siRNA gene-silencing technique, we showed that HSP27 knockdown of proliferating MRC-5 led to G_2 arrest with concurrent down-regulation of the same six genes (Fig. 2) and up-regulation of the transcriptional repressor complex E2F-4/p130 (Fig. 3). We further showed that the G_2 arrest as well as the down-regulation of the six cell cycle-related genes induced by HSP27 knockdown was prevented by concomitant knockdown of E2F-4 or p130 (Fig. 4). Because HSP27 is known to enhance the intracellular protein degradation through ubiquitination and proteosomal degradation (7, 8), we considered that HSP27 might promote the degradation of E2F-4 and/or p130. However, by a protein chase assay using cycloheximide, we observed no slowing down of E2F-4 or p130 degradation by HSP27 knockdown (Fig. 3). Collectively, HSP27 plays a pivotal role in G_2 progression of MRC-5 by up-regulating the G_2/M-associated genes via down-regulation of E2F-4/p130.

Although the mechanism(s) of down-regulation of E2F-4/p130 by HSP27 remains unclear at present, HSP27 may have an effect on the promoter activity of these molecules, because HSP27 has been reported to bind some transcriptions factors and enhance their activities (32). Indeed, we detected a significant increase of the p130 promoter activity in HSP27-knockdown MRC-5 (Fig. S2). We also found the presence of HSP27 in the nucleus of phosphorylated histone H3–positive M-phase cells (Fig. S2). These results are consistent with a notion that HSP27 negatively regulates the transcription of p130.

The cell cycle arrest of proliferating cells occurs under unfavorable conditions such as starvation and DNA damage. Starvation induces G_1 arrest (33), whereas DNA damage induces G_2 arrest (34). Furthermore, there are two types of cell cycle arrest: reversible and irreversible. The former is called quiescence, whereas the latter senescence (35). The cellular senescence is controlled by two signaling pathways; one is the p53 to $p21^{Cip1}$ pathway, and the other is the p16 to phosphorylated retinoblastoma protein pathway (36). Yet, another signaling pathway that does not involve p53 or p16 has been recently described in fibroblasts (37). In this case, the accumulation of GATA4, which is digested by autophagy in physiological conditions, activates the transcription factor NF-κB to initiate the expression of inflammatory cytokines and cellular senescence (37). Furthermore, whereas 2 days of cell cycle arrest *in vitro* can be reversible, cell cycle arrest may be irreversible after 3–4 days (38, 39). Reversible cell cycle arrest is converted to irreversible senescence through a process called geroconversion, a futile growth activity during the cell cycle arrest, which is mainly regulated by mammalian target of rapamycin (mTOR) signaling (39, 40). Senescent cells are also known to exhibit senescence-associated secretory phenotype (SASP) by producing inflammatory cytokines, metalloproteinases, and growth factors (41, 42). The SASP phenotype is initiated by NF-κB and p38 MAPK signaling (43) and maintained in an autocrine fashion by the SASP factor IL-1α (44). The production of various SASP factors is considered to be beneficial for the host by promoting immune clearance of damaged cells and preventing proliferation of potential cancer cells (45, 46). However, the SASP factors may also exacerbate age-related diseases, such as atherosclerosis (47) and type 2 diabetes mellitus (42).

In the present study, we also observed cellular senescence in MRC-5 on day 3 after HSP27 knockdown, as evidenced by positivity of senescence-associated β-gal and production of proinflammatory cytokines (Fig. 5). Although mTOR is considered to play a key role in the conversion from quiescence to senescence (39, 40), we detected no significant increase in the mTOR activity by HSP27 knockdown, as shown by immunoblot of the mTOR substances, phospho-p70 S6 kinase and phospho-4E-BP1 (data not shown). We also observed no significant increase of p16 (Fig. 5) or $p21^{Cip1}$ (Fig. 6) in HSP27-knockdown MRC-5. Thus, the cellular senescence induced by HSP27 knockdown in MRC-5 may be independent of mTOR, the p53/p21 pathway, or the p16 pathway. Because the cellular senescence induced by HSP27 knockdown was also suppressed by the concurrent knockdown of E2F-4 or p130, the G_2 arrest induced by up-regulation of E2F-4/p130 may eventually lead to cellular senescence in MRC-5 by still unknown mechanisms.

In conclusion, we have demonstrated that HSP27 promotes cell cycle progression of MRC-5 by negatively regulating E2F-4/p130 expression. Increased expression of E2F-4/p130 in HSP27-knockdown MRC-5 leads to G_2 arrest by down-regulating the expression of the six G_2/M-related genes (*CCNA2*, *CCNB1*, *CCNB2*, *CDC25C*, *CDCA3*, and *CDK1*). The G_2 arrest induced by up-regulation of E2F-4/p130 eventually results in cellular senescence in MRC-5. Thus, HSP27 may indirectly prevent cellular senescence by preventing up-regulation of E2F-4/p130. By data mining of NCBI's Gene Expression Omnibus microarray database, we indeed found decrease of HSP27 mRNA in some senescence cells: liver stellate cells (48) and premalignant lung cells (49). At present, we do not know how HSP27 negatively regulates the E2F-4/p130 expression, but the transcriptional regulation may be partly involved (Fig. S2). It also remains to be seen whether the promoting effect of HSP27 on cell cycle progression is a general phenomenon or cell type–specific phenomenon; in HSP27 knockdown in normal human lung fibroblast (NHLF) and lung adenocarcinoma cell line A549, we found that p130 mRNA levels were increased in both cell lines, whereas E2F-4 levels of NHLF or A549 were unchanged or slightly increased, respectively (Fig. S4). This suggests that the promoting effect of HSP27 on cell cycle progression is general.

Table 1
Primers and siRNAs used for this study

	Forward	Reverse
Primer		
HSP27	TCCCTGGATGTCAACCACTTC	TCTCCACCACGCCATCCT
Cyclin A2	GGTACTGAAGTCCGGGAACC	TGAACGCAGGCTGTTTACTG
Cyclin B1	TACTGGGTCGGGAAGTCACT	AGCATCTTCTTGGGCACACA
Cyclin B2	CCAGAGCAGCACAAGTAGCT	GAGAAGGACCCTTTGGAGCC
Cyclin D1	GGCGGAGGAGAACAAACAGA	CTCCTCAGGTTCAGGCCTTG
Cyclin D2	TGCAGAAGGACATCCAACCC	GCCAAGAAACGGTCCAGGTA
Cyclin D3	TGCACATGATTTCCTGGCCT	TCATGGATGGCGGGTACATG
Cyclin E1	GGAAGAGGAAGGCAAACGTGA	TTATTGTCCCAAGGCTGGCTC
CDC25c	ACTGCCACTCAGCTTACCAC	AGCTGTGCTGGGCTACATTT
cdcA3	TTCACCTAGTGCTGGCATCC	TAGGAGAGCGGGGATCTGAG
CDK1	CTGGGGTCAGCTCGTTACTC	GGAGTGCCCAAAGCTCTGAA
CDK2	TCAAGCTGCTGGATGTCATTCA	CAGTGAGAGCAGAGGCATCCAT
$p21^{Cip1}$	CTGGAGACTCTCAGGGTCGAA	CAGGACTGCAGGCTTCCTGT
$p27^{Kip1}$	TTGGAGAAGCACTGCAGAGACA	TCCACCTCTTGCCACTCGTACT
p16	CCCAACGCACCGAATAGTTA	ACCAGCGTGTCCAGGAAG
E2F-4	GGAAGCCTCACGTCCAAATA	TGAGCTCACCACTGTCCTTG
E2F-5	GTGGCTACAGCAAAGCATCA	TGGCCAAAAGTGTATCACCA
E2F-6	CAGGCCTTCCATGAACAGAT	CCTGCTCCACTTCACACAAA
E2F-7	AGGCCAAGCAGAAAACAGAA	TCCACACCAAGACTGACAGC
E2F-8	AGTGCTGTGAGCCCTGAGAT	TTCGACTTGGTTGGGATTTC
RB1	GAACATCGAATCATGGAATCCCT	AGAGGACAAGCAGATTCAAGGTGAT
p107	CCCCGCACAAGAATGGGTCAGG	ACAGACGCGTTTGGCAGGGG
p130	ATTTGGCATGGAAACCAGAG	ATCTGCCCTTTCCAGGTTCT
IL-1α	CGCCAATGACTCAGAGGAAGA	AGGGCGTCATTCAGGATGAA
IL-1β	AATCTGTACCTGTCCTGCGTGTT	TGGGTAATTTTTGGGATCTACACTCT
IL-6	GGTACATCCTCGACGGCATCT	GTGCCTCTTTGCTGCTTTCAC
IL-8	CTTGGCAGCCTTCCTGATTT	TTCTTTAGCACTCCTTGGCAAAA
β-Actin	GGACATCCGCAAAGACCTGTA	TGCATCCTGTCGGCAATG
GAPDH	GATTCCACCCATGGCAAATT	GATGGTGATGGGATTTCCATTG
siRNA		
HSP27	UGAGAGACUGCCGCCAAGUAA	UUACUUGGCGGCAGUCUCAUU
E2F-4a[a]	GCGGCGGAUUUACGACAUUdTdT	AAUGUCGUAAAUCCGCCGCdTdT
E2F-4b	GGCAGAGAUCGAGGAGCUGdTdT	CAGCUCCUCGAUCUCUGCCdTdT
p130a[a]	GAGCAGAGCUUAAUCGAAUUU	AAAUUCGAUUAAGCUCUGCUC
p130b	UACUUUAUAGUAAAGCAUCUC	GAUGCUUUACUAUAAAGUAUU
Control	UUCUCCGAACGUGUCACGUdTdT	ACGUGACACGUUCGGAGAAdTdT

[a] We prepared two siRNA sets for E2F-4 and p130 and confirmed similar results. E2F-4a and p130a siRNA were chosen for further study.

Experimental procedures

Cell culture and treatment

MRC-5 was obtained from Riken Cell Bank (Tsukuba, Japan) and maintained in Dulbecco's modified Eagle's medium (Sigma-Aldrich) supplemented with 5% FBS, streptomycin (100 μg/ml) and penicillin (100 units/ml) at 37 °C in 5% CO_2. To synchronize the cell cycle, cells were cultured in a 24-well plate to <70% confluence, washed with PBS, and placed in serum-free Dulbecco's modified Eagle's medium for 24 h. Then FBS was added to the medium to make the final concentration of 5%. DNA damage was induced in cells by exposing to UV light (λ = 253.7 nm, 120 microwatts cm^{-2}) for 15 min and culturing for 4 h.

Immunoblot analysis

Cells were washed with PBS and solubilized with CelLytic M® (Sigma-Aldrich) containing Protease Inhibitor Mixture Complete® (Roche Diagnostics, Mannheim, Germany) and Phosphatase Inhibitor Mixture® (Toyobo, Osaka, Japan). After 15 min of mixing at room temperature, cell debris was removed by centrifugation. In some experiments, nuclear and cytosolic fractions were prepared by using the NucBaster™ protein extraction kit (Merck Millipore, Billerica, MA), following the manufacturer's instructions. Samples were electrophoresed on an SDS-polyacrylamide gel under reducing conditions and electrophoretically blotted onto a polyvinylidene difluoride membrane. Membranes were blocked in 5% skim milk and probed with a primary antibody. Mouse antibodies against α-tubulin and β-actin were obtained from Sigma-Aldrich; goat anti-HSP27 antibody, rabbit anti-E2F-4 antibody, rabbit anti-glyceraldehyde-3-phosphate dehydrogenase (GAPDH), rabbit anti-p53 antibodies, and mouse anti-ubiquitin antibody were from Santa Cruz; mouse mAbs against p130, RB1, and $p21^{Cip1}$ were from BD Biosciences; and rabbit polyclonal antibodies against phospho-HSP27 (Ser-82), cyclin B1, p130, p16, and histone H3 were from Cell Signaling (Beverly, MA). After washing, membranes were reacted with a horseradish peroxidase–conjugated secondary antibody and developed using Luminata™ Forte Western HRP Substrate (Merck Millipore). Signal intensities were quantified using ImageJ software (National Institutes of Health, Bethesda, MD). Protein carbonylation, a major form of protein oxidation, was determined using an Oxiselect™ protein carbonyl immunoblot kit (Cell Biolabs Inc., San Diego, CA) following the manufacturer's instructions.

siRNA transfection

The siRNAs listed in Table 1 were obtained from GeneDesign (Osaka, Japan). Transfection of siRNA was performed by Lipofectamine RNAiMax (Invitrogen). Briefly, cells were suspended in 5% FBS Opti-MEM (Thermo Fisher Scientific) and seeded in a 12-well plate at 2×10^4 cells/ml. After 24 h of culture, Lipofectamine RNAiMax siRNA complex was added to

cells. The final siRNA concentration in each well was 20 nM. The HSP27 siRNA that we used in this study has been extensively used by many previous studies as the accepted standard HSP27 siRNA (50–52) and was also found to be most effective in this study (data not shown). The results obtained by E2F-4a siRNA and p130a siRNA were shown in this paper, whereas the data obtained by E2F-4b siRNA and p130b siRNA reproduced the results by E2F-4a siRNA and p130a siRNA, respectively (data not shown). In some experiments, cells were treated with 20 μM cycloheximide (Sigma-Aldrich) or with 10 μM pifithrin-α (Cayman Chemical, Ann Arbor, MI). The pifithrin-α concentration used was predetermined by its protective effect against doxorubicin or 5-fluorourasil–induced cell growth inhibition (53) (Fig. S3). Cell lysates for immunoblot analysis were prepared as stated above.

Cell proliferation assay

Cells were seeded in a 96-well plate and transfected with control siRNA or HSP27 siRNA. Cell numbers were quantified by Cell Counting Kit-8 (CCK8; Dojindo Laboratory, Kumamoto, Japan). In brief, we added 10 μl of CCK8 reagent to each well and incubated for 1 h. Then the medium from each well was transferred to a new 96-well plate. Optical density at 450 nm was measured on a microplate reader (ARVO, PerkinElmer Life Sciences).

Cell counting and cell cycle analysis by MUSE

Cells in a 12-well plate were transfected with siRNA and cultured for 2 days. Then cells were harvested by trypsin-EDTA and centrifuged at 100 $\times$ *g* for 5 min. Cell pellets were resuspended in 330 μl of PBS. A portion of the cell suspension (30 μl) was mixed with the Muse Count & Viability Kit (Millipore) to determine cell numbers and viability using the MUSE cell analyzer (Millipore). The remaining cell suspension (300 μl) was mixed with 700 μl of ethanol and fixed at −20 °C for 4 h. After washing twice with PBS, cells were suspended in the Muse cell cycle kit (Millipore), and the cell cycles were determined using the MUSE cell analyzer.

Quantitative PCR

Total RNAs were extracted from cells using the RNeasy Mini Kit (Qiagen). RNA samples (500 ng each) were reverse-transcribed using the High Capacity RNA-to-cDNA Kit (Applied Biosystems, Foster City, CA). Quantitative PCR was performed using THUNDERBIRD® SYBR® qPCR mix (Toyobo, Osaka, Japan) and the ABI Step One real-time PCR system with β-actin or GAPDH as a reference control. The sequences of the sense and antisense primers used for amplification are listed in Table 1.

Immunocytochemistry

Cells were cultured in a multiwell glass chamber plate (BD Falcon, Franklin Lakes, NJ), washed with PBS, and fixed with ice-cold ethanol at −20 °C for 4 min. After washing, cells were treated with Dakocytomation Protein Block (Dako, Glostrup, Denmark) for 1 h. Then cells were incubated with anti-E2F-4 or anti-p130 antibody. After washing, cells were incubated with Alexa 488 or Alexa 555 fluorescein-labeled secondary antibodies (Invitrogen) and DNA staining reagent To-PRO3 (Invitrogen). After washing and mounting, images were taken by confocal laser microscope (Carl Zeiss GmBH, Jena, Germany).

Cytochemical staining for β-gal

Cells in a 24-well plate were fixed with 4% paraformaldehyde at room temperature for 15 min. After washing with PBS, cells were incubated in a β-gal staining solution (100 mM sodium phosphate buffer, pH 6.0, 2 mM $MgCl_2$, 5 mM potassium ferricyanide, 5 mM potassium ferrocyanide, and 1 mg/ml X-gal). After incubation at 37 °C for 18 h, cells were washed with PBS and counterstained with 1 μg/ml 4′,6-diamidino-2-phenylindole. Four images were taken randomly, and total and β-gal–positive blue cells were counted by ImageJ software.

To detect whether senescence cells were at the G_2 phase, fluorometric senescence cell detection reagent SPiDER-βGal® (Dojindo Laboratory) was used. One day after control and HSP27 siRNA transfection, cells were detached, seeded in an 8-well chamber slide (BD Falcon), and cultured an additional 2 days. After washing, cells were fixed with 4% paraformaldehyde and treated with SPiDER-βGal®, following the manufacturer's instructions. After incubation with this reagent, cells were fixed again and then stained with Ki-67 (Abcam, Cambridge, UK) or cyclin B1 (Cell Signaling) antibodies, which were visualized with Alexa 633 fluorescein-labeled secondary antibody (Invitrogen) and under confocal microscopy.

Statistical analysis

Quantitative data are presented as the mean ± S.E. Statistical analysis was performed using Student's *t* test. $p < 0.05$ was considered statistically significant.

Author contributions—A.-M. P. conceptualization; A.-M. P., I. T., and O. Y. funding acquisition; A.-M. P. investigation; A.-M. P. methodology; A.-M. P. writing-original draft; A.-M. P. project administration; I. T. and O. Y. supervision; I. T. and O. Y. writing-review and editing; O. Y. resources.

Acknowledgment—We thank Namie Sakiyama for excellent technical assistance.

References

1. Garrido, C., Paul, C., Seigneuric, R., and Kampinga, H. H. (2012) The small heat shock proteins family: the long forgotten chaperones. *Int. J. Biochem. Cell Biol.* **44,** 1588–1592 CrossRef Medline
2. Arrigo, A. (2017) Mammalian HspB1 (Hsp27) is a molecular sensor linked to the physiology and environment of the cell. *Cell Stress Chaperones* **22,** 517–529 CrossRef Medline
3. Rocchi, P., Jugpal, P., So, A., Sinneman, S., Ettinger, S., Fazli, L., Nelson, C., and Gleave, M. (2006) Small interference RNA targeting heat-shock protein 27 inhibits the growth of prostatic cell lines and induces apoptosis via caspase-3 activation *in vitro*. *BJU Int.* **98,** 1082–1089 CrossRef Medline
4. Hayashi, N., Peacock, J. W., Beraldi, E., Zoubeidi, A., Gleave, M. E., and Ong, C. J. (2012) Hsp27 silencing coordinately inhibits proliferation and promotes Fas-induced apoptosis by regulating the PEA-15 molecular switch. *Cell Death Differ.* **19,** 990–1002 CrossRef Medline
5. Wettstein, G., Bellaye, P. S., Micheau, O., and Bonniaud, P. (2012) Small heat shock proteins and the cytoskeleton: an essential interplay for cell integrity? *Int. J. Biochem. Cell Biol.* **44,** 1680–1686 CrossRef Medline
6. Christians, E. S., Ishiwata, T., and Benjamin, I. J. (2012) Small heat shock proteins in redox metabolism: implications for cardiovascular diseases. *Int. J. Biochem. Cell Biol.* **44,** 1632–1645 CrossRef Medline

7. Parcellier, A., Schmitt, E., Gurbuxani, S., Seigneurin-Berny, D., Pance, A., Chantôme, A., Plenchette, S., Khochbin, S., Solary, E., and Garrido, C. (2003) HSP27 is a ubiquitin-binding protein involved in I-κBα proteasomal degradation. *Mol. Cell. Biol.* **23,** 5790–5802 CrossRef Medline
8. Parcellier, A., Brunet, M., Schmitt, E., Col, E., Didelot, C., Hammann, A., Nakayama, K., Nakayama, K. I., Khochbin, S., Solary, E., and Garrido, C. (2006) HSP27 favors ubiquitination and proteasomal degradation of $p27^{Kip1}$ and helps S-phase re-entry in stressed cells. *FASEB J.* **20,** 1179–1181 CrossRef Medline
9. Garrido, C., Brunet, M., Didelot, C., Zermati, Y., Schmitt, E., and Kroemer, G. (2006) Heat shock proteins 27 and 70: anti-apoptotic proteins with tumorigenic properties. *Cell Cycle* **5,** 2592–2601 CrossRef Medline
10. Wu, J., Liu, T., Rios, Z., Mei, Q., Lin, X., and Cao, S. (2017) Heat shock proteins and cancer. *Trends Pharmacol. Sci.* **38,** 226–256 CrossRef Medline
11. Bukrinsky, M., and Zhao, Y. (2004) Heat-shock proteins reverse the G_2 arrest caused by HIV-1 viral protein R. *DNA Cell Biol.* **23,** 223–225 CrossRef Medline
12. Acunzo, J., Andrieu, C., Baylot, V., So, A., and Rocchi, P. (2014) Hsp27 as a therapeutic target in cancers. *Curr. Drug Targets* **15,** 423–431 CrossRef Medline
13. Horman, S., Fokan, D., Mosselmans, R., Mairesse, N., and Galand, P. (1999) Anti-sense inhibition of small-heat-shock-protein (HSP27) expression in MCF-7 mammary-carcinoma cells induces their spontaneous acquisition of a secretory phenotype. *Int. J. Cancer* **82,** 574–582 CrossRef Medline
14. O'Callaghan-Sunol, C., Gabai, V. L., and Sherman, M. Y. (2007) Hsp27 modulates p53 signaling and suppresses cellular senescence. *Cancer Res.* **67,** 11779–11788 CrossRef Medline
15. Park, A.-M., Kanai, K., Itoh, T., Sato, T., Tsukui, T., Inagaki, Y., Selman, M., Matsushima, K., and Yoshie, O. (2016) Heat shock protein 27 plays a pivotal role in myofibroblast differentiation and in the development of bleomycin-induced pulmonary fibrosis. *PLoS One* **11,** e0148998 CrossRef Medline
16. Jacobs, J. P., Jones, C. M., and Baille, J. P. (1970) Characteristics of a human diploid cell designated MRC-5. *Nature* **227,** 168–170 CrossRef Medline
17. Schafer, K. A. (1998) The cell cycle: a review. *Vet. Pathol.* **35,** 461–478 CrossRef Medline
18. Schwartz, G. K., and Shah, M. A. (2005) Targeting the cell cycle: a new approach to cancer therapy. *J. Clin. Oncol.* **23,** 9408–9421 CrossRef Medline
19. Müller, G. A., and Engeland, K. (2010) The central role of CDE/CHR promoter elements in the regulation of cell cycle-dependent gene transcription. *FEBS J.* **277,** 877–893 CrossRef Medline
20. van den Heuvel, S., and Dyson, N. J. (2008) Conserved functions of the pRB and E2F families. *Nat. Rev. Mol. Cell Biol.* **9,** 713–724 CrossRef Medline
21. Hans, F., and Dimitrov, S. (2001) Histone H3 phosphorylation and cell division. *Oncogene* **20,** 3021–3027 CrossRef Medline
22. He, S., and Sharpless, N. E. (2017) Senescence in health and disease. *Cell* **169,** 1000–1011 CrossRef Medline
23. Scholzen, T., and Gerdes, J. (2000) The Ki-67 protein: from the known and the unknown. *J. Cell. Physiol.* **182,** 311–322 CrossRef Medline
24. Lindqvist, A., van Zon, W., Karlsson Rosenthal, C., and Wolthuis, R. M. (2007) Cyclin B1-Cdk1 activation continues after centrosome separation to control mitotic progression. *PLoS Biol.* **5,** e123 CrossRef Medline
25. Georgakilas, A. G., Martin, O. A., and Bonner, W. M. (2017) p21: a two-faced genome guardian. *Trends Mol. Med.* **23,** 310–319 CrossRef Medline
26. Gudkov, A. V., and Komarova, E. A. (2005) Prospective therapeutic applications of p53 inhibitors. *Biochem. Biophys. Res. Commun.* **331,** 726–736 CrossRef Medline
27. Vermeulen, K., Van Bockstaele, D. R., and Berneman, Z. N. (2003) The cell cycle: a review of regulation, deregulation and therapeutic targets in cancer. *Cell Prolif.* **36,** 131–149 CrossRef Medline
28. Williams, G. H., and Stoeber, K. (2012) The cell cycle and cancer. *J. Pathol.* **226,** 352–364 CrossRef Medline
29. Kang, C., Xu, Q., Martin, T. D., Li, M. Z., Demaria, M., Aron, L., Lu, T., Yankner, B. A., Campisi, J., and Elledge, S. J. (2015) The DNA damage response induces inflammation and senescence by inhibiting autophagy of GATA4. *Science* **349,** aaa5612 CrossRef Medline
30. Macaluso, M., Montanari, M., and Giordano, A. (2006) Rb family proteins as modulators of gene expression and new aspects regarding the interaction with chromatin remodeling enzymes. *Oncogene* **25,** 5263–5267 CrossRef Medline
31. Litovchick, L., Sadasivam, S., Florens, L., Zhu, X., Swanson, S. K., Velmurugan, S., Chen, R., Washburn, M. P., Liu, X. S., and DeCaprio, J. A. (2007) Evolutionarily conserved multisubunit RBL2/p130 and E2F4 protein complex represses human cell cycle-dependent genes in quiescence. *Mol. Cell.* **26,** 539–551 CrossRef Medline
32. Friedman, M. J., Li, S., and Li, X. (2009) Activation of gene transcription by heat shock protein 27 may contribute to its neuronal protection. *J. Biol. Chem.* **284,** 27944–27951 CrossRef Medline
33. Krizhanovsky, V., Yon, M., Dickins, R. A., Hearn, S., Simon, J., Miething, C., Yee, H., Zender, L., and Lowe, S. W. (2008) Senescence of activated stellate cells limits liver fibrosis. *Cell* **134,** 657–667 CrossRef Medline
34. Plesca, D., Crosby, M. E., Gupta, D., and Almasan, A. (2007) E2F4 function in G_2: maintaining G_2-arrest to prevent mitotic entry with damaged DNA. *Cell Cycle* **6,** 1147–1152 CrossRef Medline
35. Gire, V., and Dulic, V. (2015) Senescence from G_2 arrest, revisited. *Cell Cycle* **14,** 297–304 CrossRef Medline
36. Campisi, J., and d'Adda di Fagagna, F. (2007) Cellular senescence: when bad things happen to good cells. *Nat. Rev. Mol. Cell Biol.* **8,** 729–740 CrossRef Medline
37. Thurlings, I., and de Bruin, A. (2016) E2F transcription factors control the roller coaster ride of cell cycle gene expression. *Methods Mol. Biol.* **1342,** 71–88 CrossRef Medline
38. Campisi, J. (2013) Aging, cellular senescence, and cancer. *Annu. Rev. Physiol.* **75,** 685–705 CrossRef Medline
39. Blagosklonny, M. V. (2014) Geroconversion: irreversible step to cellular senescence. *Cell Cycle* **13,** 3628–3635 CrossRef Medline
40. Terzi, M. Y., Izmirli, M., and Gogebakan, B. (2016) The cell fate: senescence or quiescence. *Mol. Biol. Rep.* **43,** 1213–1220 CrossRef Medline
41. Leontieva, O. V., Lenzo, F., Demidenko, Z. N., and Blagosklonny, M. V. (2012) Hyper-mitogenic drive coexists with mitotic incompetence in senescent cells. *Cell Cycle* **11,** 4642–4649 CrossRef Medline
42. Tchkonia, T., Zhu, Y., van Deursen, J., Campisi, J., and Kirkland, J. L. (2013) Cellular senescence and the senescent secretory phenotype: therapeutic opportunities. *J. Clin. Invest.* **123,** 966–972 CrossRef Medline
43. Salminen, A., Kauppinen, A., and Kaarniranta, K. (2012) Emerging role of NF-κB signaling in the induction of senescence-associated secretory phenotype (SASP). *Cell. Signal.* **24,** 835–845 CrossRef Medline
44. Orjalo, A. V., Bhaumik, D., Gengler, B. K., Scott, G. K., and Campisi, J. (2009) Cell surface-bound IL-1α is an upstream regulator of the senescence-associated IL-6/IL-8 cytokine network. *Proc. Natl. Acad. Sci. U.S.A.* **106,** 17031–17036 CrossRef Medline
45. Xue, W., Zender, L., Miething, C., Dickins, R. A., Hernando, E., Krizhanovsky, V., Cordon-Cardo, C., and Lowe, S. W. (2007) Senescence and tumour clearance is triggered by p53 restoration in murine liver carcinomas. *Nature* **445,** 656–660 CrossRef Medline
46. Rodier, F., and Campisi, J. (2011) Four faces of cellular senescence. *J. Cell Biol.* **192,** 547–556 CrossRef Medline
47. Zhou, X., Perez, F., Han, K., and Jurivich, D. A. (2006) Clonal senescence alters endothelial ICAM-1 function. *Mech. Ageing Dev.* **127,** 779–785 CrossRef Medline
48. Shin, J. S., Hong, S. W., Lee, S. L., Kim, T. H., Park, I. C., An, S. K., Lee, W. K., Lim, J. S., Kim, K. I., Yang, Y., Lee, S. S., Jin, D. H., and Lee, M. S. (2008) Serum starvation induces G_1 arrest through suppression of Skp2-CDK2 and CDK4 in SK-OV-3 cells. *Int. J. Oncol.* **32,** 435–439 Medline
49. Collado, M., Gil, J., Efeyan, A., Guerra, C., Schuhmacher, A. J., Barradas, M., Benguría, A., Zaballos, A., Flores, J. M., Barbacid, M., Beach, D., and Serrano, M. (2005) Tumour biology: senescence in premalignant tumours. *Nature* **436,** 642 CrossRef Medline
50. Zhu, Z., Xu, X., Yu, Y., Graham, M., Prince, M. E., Carey, T. E., and Sun, D. (2010) Silencing heat shock protein 27 decreases metastatic behavior of human head and neck squamous cell cancer cells *in vitro*. *Mol. Pharm.* **7,** 1283–1290 CrossRef Medline

51. Deng, W., Zhang, Y., Gu, L., Cui, J., Duan, B., Wang, Y., and Du, J. (2016) Heat shock protein 27 downstream of P38-PI3K/Akt signaling antagonizes melatonin-induced apoptosis of SGC-7901 gastric cancer cells. *Cancer Cell Int.* **16,** 5 CrossRef Medline
52. Burban, A., Sharanek, A., Hüe, R., Gay, M., Routier, S., Guillouzo, A., and Guguen-Guillouzo, C. (2017) Penicillinase-resistant antibiotics induce non-immune-mediated cholestasis through HSP27 activation associated with PKC/P38 and PI3K/AKT signaling pathways. *Sci. Rep.* **7,** 1815 CrossRef Medline
53. Liu, X., Chua, C. C., Gao, J., Chen, Z., Landy, C. L., Hamdy, R., and Chua, B. H. (2004) Pifithrin-α protects against doxorubicin-induced apoptosis and acute cardiotoxicity in mice. *Am. J. Physiol. Heart Circ. Physiol.* **286,** H933–H939 CrossRef Medline